to electron-exchange interactions (J_e) of the same absolute value ($\sim$0.014 cm^{-1}) but opposite in sign. The magnitude of J_e for the Gd(III)-Ru(III) dimer is more than ten times greater than that for the homogeneous Gd(III)-Gd(III) dimer.[3] (For the Gd(III)-Gd(III) center in $CsMgCl_3$, J_e is about 0.0011 cm^{-1}.) This result is consistent with the view that the d electrons of the transition-metal ions are considerably more delocalized than the f electrons of the rare-earth ions. The strength of the exchange coupling in the homogeneous Ru(III)-Ru(III) dimer is not known; however, the interactions in other d-electron systems such as the Cr(III)-Cr(III), Cr(III)-Mo(III), and Mo(III)-Mo(III) centers fall in the 1 to 3 cm^{-1} range.[5,7]

In summary, the Gd(III)-Ru(III) center in $CsMgCl_3$ has been shown to be a weakly coupled magnetic dimer where the g values of the two ions have opposite signs. The electron-exchange interactions are in the order of 0.014 cm^{-1}, but it is not clear if the coupling is ferromagnetic or antiferromagnetic.

Registry No. Gd(III), 22541-19-1; Ru(III), 22541-88-4; $CsMgCl_3$, 13845-09-5.

Models of the Cytochromes *b*. 5. EPR Studies of Low-Spin Iron(III) Tetraphenylporphyrins

F. Ann Walker,*[1] David Reis, and Virginia L. Balke

Contribution from the Department of Chemistry, San Francisco State University, San Francisco, California 94132. *Received February 13, 1984*

Abstract: The EPR spectra of a wide range of tetraphenylporphyrin complexes of Fe(III) have been investigated as a function of solvent, ligand type, ligand basicity, porphyrin substituents, covalent attachment of axial ligands, and mixed axial ligand coordination. The results show the following: (1) EPR parameters of low-spin bis-axial ligand complexes of Fe(III) porphyrins depend not only on ligand basicity but also on ligand type. Of the three major classes studied, bis(imidazole) and -(aminopyridine) complexes all have similar values of g_x, g_y, and g_z which are nearly independent of ligand basicity, while bis(pyrazole) (and bis(indazole)) complexes have g_x, g_y, and g_z values which tend to converge as ligand basicity increases. (2) The effect of the electron-donating or -withdrawing nature of phenyl substituents on the EPR parameters of a large series of phenyl-substituted (TPP)Fe(N-MeIm)$_2^+$ derivatives is very small: The rhombicity $V/\Delta = 0.64 \pm 0.01$ for all complexes, while the tetragonality Δ/λ ranges from 2.97 for electron-donating substituents to 3.33 for electron-withdrawing substituents, the opposite trend from that expected for increasing axial ligand donor strength. No difference was observed in the EPR parameters of unsymmetrically as compared to symmetrically substituted TPP derivatives. (3) Covalent attachment of axial ligands or steric crowding of externally supplied axial ligands in the hope of seeing variation in the EPR parameters with relative axial ligand plane orientation (parallel vs. perpendicular) was not successful in producing pure isomers, and thus no effects on EPR parameters with axial ligand plane orientation were detected. (4) A covalently attached (N-alkylimidazole-TPP)Fe(III) derivative was utilized to allow formation of mixed-ligand low-spin Fe(III) complexes. The alkylimidazole-imidazolate ligand combination was only very slightly more tetragonal than its protonated imidazole counterpart, while the alkylimidazole-pyrazole, 3-aminopyrazole, 1,2,4-triazole, and 2-methylimidazole mixed ligand complexes all had EPR parameters uniquely different from those of the parent bis-ligand complexes. Discussion of these results in light of the g values of membrane-bound cytochromes *b*, *c*, and a_3 bound to cyanide is also included.

EPR spectroscopy has for many years been one of the most useful tools for characterizing ferric hemoproteins[2-52] and model hemins.[14,53-67] Of the three EPR-active spin states ($S = {}^5/_2, {}^3/_2$, and ${}^1/_2$), the low-spin ferriheme proteins have been studied in most

(1) Recipient of the NIH Research Career Development Award, 1976-81.
(2) Griffith, J. S. *Proc. R. Soc. London, Ser. A* **1956**, *235A*, 23-26.
(3) Gibson, J. F.; Ingram, D. J. E.; Schonland, D. *Discuss. Faraday Soc.* **1958**, *26*, 72-95.
(4) Kotani, M. *Suppl. Prog. Theor. Phys.* **1961**, *17*, 4-13.
(5) Kotani, M. *Rev. Mod. Phys.* **1963**, *35*, 717-723.
(6) Griffith, J. S. *Biopolymers, Symp. 1* **1964**, 35-46.
(7) Kotani, M. *Biopolymers, Symp. 1* **1964**, 67-73.
(8) Harris, G. *Theor. Chim. Acta* **1966**, *5*, 379-397.
(9) Weissbluth, M. *Struct. Bonding (Berlin)* **1967**, *2*, 1-125.
(10) Mizuhashi, S. *J. Phys. Soc. Jpn.* **1969**, *26*, 468-492.
(11) Loew, G. M. H. *Biophys. J.* **1970**, *10*, 196-212.
(12) Blumberg, W. E.; Peisach, J. *Adv. Chem. Ser.* **1971**, *100*, 271-291.
(13) Peisach, J.; Blumberg, W. E.; Ogawa, S.; Rachmilewitz, E. A.; Oltzik, R. *J. Biol. Chem.* **1971**, *246*, 3342-3355.
(14) Peisach, J.; Blumberg, W. E.; Adler, A. D. *Ann. N.Y. Acad. Sci.* **1973**, *206*, 310-327.
(15) Taylor, C. P. S. *Biochim. Biophys. Acta* **1977**, *491*, 137-149.
(16) Bohan, T. L. *J. Magn. Reson.* **1977**, *26*, 109-118.
(17) Caro, P.; Faucher, M.; Savy, M.; Pankowska, H. *J. Chem. Phys.* **1978**, *68*, 1045-1057.
(18) Huynh, B. H.; Emptage, M. H.; Münck, E. *Biochim. Biophys. Acta* **1978**, *534*, 295-306.
(19) Palmer, G. In "The Porphyrins"; Dolphin, D., Ed.; Academic Press: New York, 1979; Vol. IV, pp 313-353.
(20) Smith, T. D.; Pilbrow, J. R. In "Biological Magnetic Resonance"; Berliner, L. J., Ruben, J., Eds.; Plenum Press: New York, 1980; Vol. 2, pp 85-168.
(21) Palmer, G. In "Iron Porphyrins"; Lever, A. B. P., Gray, H. B., Eds.; Addison-Wesley: Reading, MA, 1983; Part II, pp 43-88.
(22) Bois-Poltoratsky, R.; Ehrenberg, A. *Eur. J. Biochem.* **1967**, *2*, 361-365.
(23) Watari, H.; Groudinsky, O.; Labeyrie, F. *Biochim. Biophys. Acta* **1967**, *131*, 589-592.
(24) Ichikawa, Y.; Yamano, T. *Arch. Biochem. Biophys.* **1967**, *121*, 742-749.
(25) Tsai, R.; Yu, C. A.; Gunsalus, I. C.; Peisach, J.; Blumberg, W.; Orone-Johnson, W. H.; Beinert, H. *Proc. Natl. Acad. Sci. U.S.A.* **1970**, *66*, 1157-1163.
(26) Hori, H. *Biochim. Biophys. Acta* **1971**, *251*, 227-235.
(27) LeGall, J.; Bruschi-Heriaud, M.; Dervartanian, D. V. *Biochim. Biophys. Acta* **1971**, *234*, 499-512.
(28) Dervartanian, D. V.; LeGall, J. *Biochim. Biophys. Acta* **1971**, *243*, 53-65.
(29) Blumberg, W. E.; Peisach, J. In "structure and Bonding of Macromolecules and Membrane"; Chance, B., Yonetani, T., Eds.; Academic Press: New York, 1971; p 215.
(30) Yonetani, T.; Iizuka, T.; Waterman, M. R. *J. Biol. Chem.* **1971**, *246*, 7683-7689.
(31) Passon, P. G.; Reed, D. W.; Hultquist, D. E. *Biochim. Biophys. Acta* **1972**, *275*, 51-61.
(32) Seamonds, B.; Blumberg, W. E.; Peisach, J. *Biochim. Biophys. Acta* **1972**, *263*, 507-514.
(33) Peisach, J.; Appleby, C. A.; Blumberg, W. E. *Arch. Biochem. Biophys.* **1972**, *150*, 725-732.
(34) Bearden, A. J.; Morgan, W. T.; Muller-Eberhard, U. *Biochem. Biophys. Res. Commun.* **1974**, *61*, 265-272.
(35) Orme-Johnson, N. R.; Hansen, R. E.; Beinert, H. *J. Biol. Chem.* **1974**, *249*, 1922-1927.
(36) Ikeda-Saito, M.; Iizuka, T. *Biochim. Biophys. Acta* **1975**, *393*, 335-342.
(37) Appleby, C. A.; Blumberg, W. E.; Peisach, J.; Whittenberg, B. A.; Whittenberg, J. B. *J. biol. Chem.* **1976**, *251*, 6090-6096.

0002-7863/84/1506-6888$01.50/0

Table I. EPR Data for Selected Cytochromes *b* and Related Bis(imidazole)-Coordinated Proteins and Model Hemins

	g_z	g_y	g_x	Δ/λ	V/Δ	$a^2+b^2+c^2$	$\sum g^2$	ref
			Ferriheme Proteins					
"B hemichrome"	2.95	2.26	1.47	3.11	0.58	1.001	16.0	29
cytochrome b_5, liver, native	3.03	2.23	1.43	3.23	0.52	1.007	16.2	22
cytochrome b_5, erythrocyte	3.03	2.23	1.39	3.06	0.53	1.003	16.1	31
cytochrome b_2, yeast, native	2.99	2.28	1.49	3.17	0.57	1.014	16.4	23
cytochrome *a*	3.03	2.24	1.24	2.52	0.59	0.992	15.7	38
leghemoglobin LS signal 1	3.02	2.24	1.34	2.82	0.56	0.998	15.9	37
sulfite oxidase heme signal	2.92	2.25	1.53	3.39	0.56	1.002	15.9	a
cytochrome *c*-imidazole	2.96	2.30	1.58	3.43	0.57	1.022	16.6	36
hemoglobin-imidazole	2.91	2.26	1.53	3.32	0.58	1.002	15.9	26
heme-hemopexin	2.86	2.26	1.60	3.59	0.59	1.003	15.9	34
"H hemichrome"	2.80	2.26	1.67	3.91	0.60	1.004	15.7	29
cytochrome b_5, pH 11.5	2.82	2.28	1.68	3.86	0.60	1.011	16.0	22
cytochrome b_5, liver, pH 12	2.76	2.28	1.68	3.71	0.66	1.002	15.6	22
cytochrome b_2, yeast, pH 12.1	2.70	2.24	1.75	4.51	0.60	1.001	15.4	23
cytochrome c_3	2.86	2.29	1.62	3.50	0.62	1.010	16.1	28
leghemoglobin LS signal 2	2.69	2.24	1.72	4.19	0.63	0.994	15.2	37
			Model Hemins					
$(Im)_2$hemin *a*	2.96	2.29	1.48	3.02	0.61	1.008	16.2	62
$(Im)_2$protohemin in Im	3.02	2.24	1.51	3.54	0.50	1.016	16.4	14
$(Im)_2$protohemin in Im + NaOH	2.78	2.26	1.72	4.25	0.58	1.010	16.0	14
$(Im)_2$protohemin DME[a] in $CHCl_3$	2.80	2.26	1.68	3.98	0.59	1.006	15.8	57
$(Im)_2$deuterohemin	2.93	2.27	1.53	3.30	0.58	1.006	16.1	53
$((Im)_2TPP)Fe$ in $CHCl_3$/EtOH	2.923	2.296	1.556	3.26	0.61	1.012	16.2	14
$(Im)_2TCPP$ in H_2O at pH 6	2.82	~2.26	1.56	3.29	0.64	0.990	15.5	56

[a] Kessler, D. L.; Rajogopalan, K. V. *J. Biol. Chem.* **1972**, *247*, 6566.

depth. This is largely due to the fact that the EPR parameters (*g* values) may be used to calculate the relative energies of the

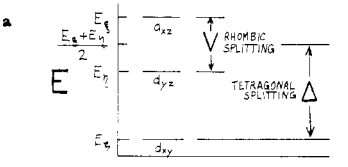

TYPE	g_z	g_y	g_x	Δ/λ (AVE.)	V/Δ (AVE.)	Ligands ... Symmetry
P	2.41	2.26	1.93	5.2	0.99	HO-Fe-S-R (H) ...most axial
O	2.55	2.17	1.85	6.6	0.53	HO-Fe-Hist.
H	2.80	2.26	1.67	3.9	0.66	Hist.-Fe-Hist. (Protein denatured)
B	2.95	2.26	1.47	3.1	0.58	Hist.-Fe-Hist.
C	3.05	2.25	1.25	2.5	0.58	Hist.-Fe-SR_2 ...most rhombic

Figure 1. (a) Orbital splitting pattern for low-spin iron(III) porphyrins. (b) Classification of types of low-spin ferriheme proteins according to axial ligands, based upon their orbital splitting pattern as calculated from EPR *g* values.

d orbitals d_{xy}, d_{xy}, and d_{yz}; from such calculations Peisach and Blumberg have developed a method of analysis which allows the identity of the axial ligands to be assigned.[12,14] The theory used to calculate the d-orbital energies was first outlined by Griffith,[2,6] elaborated in terms of real d-orbital wave functions by Kotani,[4,5,7] and later lucidly described by Weissbluth.[9] Treatments by Bohan[16] and Taylor,[15] as well as the earlier workers, have recently been summarized by Palmer in two very readable chapters.[19,21] Without reiterating the details of the theory, the salient features may be summarized as follows: The electron configuration of low-spin Fe(III) is $(d_{xy})^2(d_{xz},d_{yz})^3$, which, even in equatorially symmetrical porphyrins, exists as a rhombically distorted system as shown in Figure 1a, with tetragonal splitting parameter Δ and rhombic splitting parameter V. The two wave functions (for α and β spins) are thus linear combinations of the three states with coefficients *a* (for d_{yz}), *b* (for d_{xz}), and *c* (d_{xy}). When the axis system of Taylor[15] is used, it can be shown that

(38) Aasa, R.; Albracht, S. P. J.; Falk, K. E.; Fanne, B.; Vanngard, T. *Biochim. Biophys. Acta* **1976**, *476*, 260–272.
(39) Brautigan, D. L.; Feinberg, B. A.; Hoffman, B. M.; Margoliash, E.; Peisach, J.; Blumberg, W. E. *J. Biol. Chem.* **1977**, *252*, 574–582.
(40) Chevion, M.; Peisach, J.; Blumberg, W. E. *J. Biol. Chem.* **1977**, *252*, 3636–3645.
(41) Beinert, H. *Methods Enzymol.* **1978**, *52*, 133–150.
(42) Chao, Y.-Y. H.; Bersohn, R.; Aisen, P. *Biochemistry* **1979**, *18*, 774–779.
(43) Siedow, J. N.; Vickery, L. E.; Palmer g. *Arch. Biochem. Biophys.* **1980**, *203*, 101–197.
(44) Blum, H.; Ohnishi, T. *Biochim. Biophys. Acta* **1981**, *621*. 9–18.
(45) Hollenberg, P. F.; Hager, L. P.; Blumberg, W. E.; Peisach, J. *J. Biol. Chem.* **1980**, *255*, 4801–4807.
(46) Lipscomb, J. D. *Biochemistry* **1980**, *19*, 3490–3599.
(47) Carter, K. R.; Tsai, A.; Palmer, G. *FEBS Lett.* **1981**, *132*, 243–246.
(48) Smith, M.; McLendon, G. *J. Am. Chem. Soc.* **1981**, *103*, 4912–4921.
(49) Tsai, A.; Palmer, G. *Biochim. Biophys. Acta* **1982**, *681*, 484–495.
(50) Ellfolk, N.; Rönnberg, M.; Aasa, R.; Andreasson, L. E.; Vanngard, T. *Biochim. Biophys. Acta* **1983**, *743*, 23–30.
(51) Muhoberac, B. B.; Wharton, D. C. *J. Biol. Chem.* **1983**, *258*, 3019–3027.
(52) Migita, C. T.; Migita, K.; Iwaizumi, M. *Biochim. Biophys. Acta* **1983**, *743*, 290–298.
(53) Momenteau, M. *Biochim. Biophys. Acta* **1973**, *304*, 814–827.
(54) Momenteau, M.; Mispelter, J.; Lexa, D. *Biochim. Biophys. Acta* **1973**, *320*, 652–662.
(55) Momenteau, M.; Rougee, M.; Loock, B. *Eur. J. Biochem.* **1976**, *71*, 63–76.
(56) Stang, J. D.; Hartzell, C. R. *Bioinorg. Chem.* **1976**, *5*, 219–233.
(57) Yoshimura, T.; Ozaki, T.; Shintani, Y.; Watanabe, H. *J. Inorg. Nucl. Chem.* **1976**, *36*, 1879–1883.
(58) Yoshimura, T.; Ozaki, T.; Shintani, Y. *J. Inorg. Nucl. Chem.* **1977**, *39*, 185–190.
(59) Ruf, H. H.; Wende, P. *J. Am. Chem. Soc.* **1977**, *99*, 5499–5500.
(60) Ozaki, T.; Yoshimura, T. *Inorg. Chim. Acta* **1979**, *36*, L421–L422.
(61) Ruf, H. H.; Wende, P.; Ullrich, V. *J. Inorg. Biochem.* **1979**, *11*, 189–204.
(62) Babcock, G. T.; Van Steelandt, J.; Palmer, G.; Vickery, L.; Salmeen, I. In "Cytochrome Oxidase"; King, T. E., et al., Eds.; Elsevier: New York, 1979; pp 105–115.
(63) Stolzenberg, A. M.; Strauss, S. H.; Holm, R. H. *J. Am. Chem. Soc.* **1981**, *103*, 4763–4778.
(64) Ogoshi, H.; Sugimoto, H.; Watanabe, E.; Yoshida, Z.; Maeda, Y.; Sakai, H. *Bull. Chem. Soc. Jpn.* **1981**, *54*, 3414–3419.
(65) Migita, C. T.; Iwaizumi, M. *J. Am. Chem. Soc.* **1981**, *103*, 4378–4381.
(66) Cheng, R.; Latos-Grazynski, L.; Balch, A. L. *Inorg. Chem.* **1982**, *21*, 2412–2418.
(67) Quinn, R.; Nappa, M.; Valentine, J. S. *J. Am. Chem. Soc.* **1982**, *104*, 2588–2595.

$$a = (g_z + g_y)/4K$$
$$b = (g_z - g_x)/4K$$
$$c = (g_y - g_x)/4K \quad (1)$$

where $4K = [8(g_z + g_y - g_x)]^{1/2}$. From these quantities, a, b, and c, the relative energies of the three d orbitals of Figure 1 can be determined, and from these the tetragonal (Δ/λ) and rhombic (V/λ) splitting parameters may be calculated:[21]

$$V/\lambda = E_{yz} - E_{xz} = \frac{g_x}{g_z + g_y} + \frac{g_y}{g_z - g_x} \quad (2)$$

$$\Delta/\lambda = E_{xz} - E_{xy} - \tfrac{1}{2}V/\lambda = \frac{g_x}{g_z + g_y} + \frac{g_z}{g_y - g_x} - \tfrac{1}{2}V/\lambda$$

Peisach and Blumberg first used such equations to determine the rhombicity (V/Δ, a purely geometric factor) and tetragonality (Δ/λ, a measure of ligand donor strength) of various low-spin ferrihemes and ferriheme proteins and have found that those known to have the same axial ligands fall into very similar regions of the plot.[12,14] Five such naturally occurring ligand combinations (and five such "Regions" of V/Δ vs. Δ/λ) have been outlined, which are summarized in Figure 1b, where eq 2 is used to calculate V/Δ and $\Delta/2$,[15,19] the maximum g value is taken to be g_z,[19] and the product of the three g values is taken to be positive,[18] rather than the original definitions of Blumberg and Peisach.[12,14] As pointed out by Palmer,[21] V/Δ is allowed to be greater than two-thirds, since using the analysis of Taylor[15] means that an improper axis system is being used. More extensive studies have shown that types B and H differ in the state of protonation of the two histidines (type B have both imidazoles protonated and type H have one or both deprotonated)[14,39] and that two forms of cytochromes P_{450} (type P) exist,[40] differing in the state of protonation of the imidazole. It thus appears to be possible to assign with confidence the axial ligands of a newly discovered low-spin ferriheme protein and in many cases to know the state of protonation of the almost ubiquitous histidine ligand. As has been pointed out,[47] and as we will discuss in greater detail elsewhere,[68] however, the above generalizations do not appear to hold for low-spin heme proteins having large values of g_{max} (3.4–3.7).

In Table I are summarized the EPR parameters and calculated values of Δ/λ and V/Δ of cytochromes b_5 and b_2 and various other "B"- and "H"-type hemichromes, as well as some representative low-spin model hemins. The data of table I demonstrate that there is a range of values of g_z, g_y, and g_x observed for both types B and H hemichromes, as well as for model hemins of each type. However, because of differences in pH, buffer type, solvent, EPR spectrum resolution, and possibly also spectrometer field calibration, it is difficult to rationalize the differences in g values summarized in Table I. Possible reasons for real variations in g values among B and H hemichromes could include (a) differences in porphyrin ring substituents (i.e., cytochrome a of cytochrome oxidase vs. cytochrome b_5, or Im_2protohemin vs. Im_2hemin a or Im_2deuterohemin), (b) differences in the degree of hydrogen bonding of the imidazoles within type B hemichromes, and (c) the angular relationship of the two axial imidazole planes to each other and to the porphyrin ring substituents. In order to investigate the potential effect of each of these factors upon the EPR parameters of heme proteins we have carried out a systematic study of the EPR spectra of a series of synthetic hemins as a function of solvent, porphyrin substituents (both symmetrically and unsymmetrically placed), imidazole substituents, and axial ligand plane orientation. As a part of this study, in an attempt to place the coordination sphere of the cytochromes b in perspective and perhaps gain insight into the reasons for the almost ubiquitous involvement of imidazole as an axial ligand in heme proteins, we have investigated the EPR spectra of ferric porphyrin complexes with other azoles, pyridines, and several other six-membered ring heterocycles (see Figure 2) and mixed imidazole–L complexes, where L is an azole or pyridine.

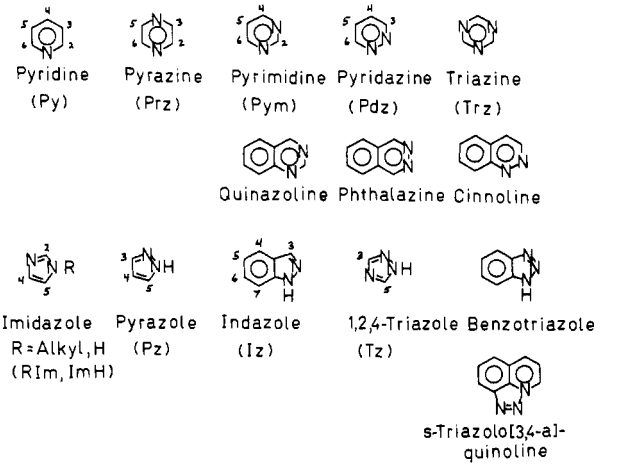

Figure 2. Classes of axial ligands used in this study.

Experimental Section

Tetraphenylporphyrin (TPP), its tetra-X-phenyl analogues (X_4TPP), and the unsymmetrically phenyl-substituted analogues (X_nY_mTPP) were prepared as described previously.[19,70] Each porphyrin was chromatographed on silica gel with benzene, benzene–petroleum ether, methylene chloride, or methylene chloride–ethyl acetate before metal insertion. Iron was inserted and the iron porphyrins were purified as described previously.[71,72]

Covalently linked imidazole TPPs were prepared from the desired ($(o\text{-}NH_2)_n$TPP)FeCl, phosgene, and 2-(*N*-imidazolyl)ethanol:[73] For the monoimidazole derivative, $[H^+ ImCH_2CH_2OCONHTPP)FeCl]Cl^-$, iron was first inserted[71] into 50 mg (0.08 mmol) of o-NH_2TPP, prepared as before.[74] It was chromatographed on silica gel and eluted with 10% MeOH/$CHCl_3$. It was evaporated to dryness, redissovled in $CHCl_3$, and reevaporated to dryness. The sample was then redissolved in 20 mL of CH_2Cl_2 plus 5 mL of pyridine, each of which had been dried over molecular sieves (Linde 4 Å). This solution was added slowly dropwise to a solution of 0.56 mL of phosgene in benzene (0.44 mol) (Aldrich) plus 20 mL of dry CH_2Cl_2 with stirring. Once the porphyrin addition was complete a solution of 157 mg of 2-(*N*-imidazolyl)ethanol (1.4 mmol), which had been prepared by the method of Traylor,[73] dissolved in 10 mL of dry CH_2Cl_2, was added dropwise. The solution was stirred overnight and then extracted 6 times with water at pH 5.0. It was then placed on a dry silica gel column and eluted with 10% methanol in $CHCl_3$.

The bis(imidazole) derivatives, called cis and trans depending upon whether the imidazole arms were attached to adjacent or opposite phenyl rings, were prepared from the *cis*- and *trans*-α,β-$(o\text{-}NH_2)_2$TPP isomers obtained by the methods outlined by Collman et al.[75] by the same general procedures as for the monoimidazole side arm complex, with the modifications that metal insertion was carried out rapidly by the method of Collman et al.[76] (no more than 10 min of heating in THF) and in dimly lit surroundings. Twice the quantities of phosgene and 2-(*N*-imidazolyl)ethanol were used in forming the six-coordinate porphyrins as compared to the monoimidazole porphyrin.

The covalently attached (ImTPP)FeCl complexes as well as the symmetrical (X_4TPP)FeCl and unsymmetrical (X_nY_mTPP)FeCl derivatives were all treated with HCl gas in dry CH_2Cl_2 and evaporated to dryness before EPR samples were prepared. This HCl treatment had the effect of protonating any amino groups present, as well as the imidazole groups of the mono and biscovalently attached imidazole derivatives. These groups are readily deprotonated upon addition of exogenous ligands more

(68) Huynh, B. H.; Walker, F. A., work in progress.
(69) Adler, A. D.; Longo, F. R.; Finarelli, J. D.; Goldmacher, J.; Assour, J.; Korsakoff, L. *J. Org. Chem.* **1967**, *32*, 476.
(70) Walker, F. A.; Balke, V. L.; McDermott, G. A. *Inorg. Chem.* **1982**, *21*, 3342–3348.
(71) Adler, A. D.; Longo, F. R.; Kampas, F.; Kim, J. *J. Inorg. Nucl. Chem.* **1970**, *32*, 2443–2448.
(72) Walker, F. A.; Balke, V. L.; McDermott, G. A. *J. Am. Chem. Soc.* **1982**, *104*, 1569–1574.
(73) Geibel, J.; Cannon, J.; Campbell, D.; Traylor, T. G. *J. Am. Chem. Soc.* **1978**, *100*, 3575–3585.
(74) Walker, F. A.; Benson, M. *J. Am. Chem. Soc.* **1980**, *102*, 5530–5538.
(75) Collman, J. P.; Gagne, R. R.; Reed, C. A.; Halbert, T. R.; Lang, G.; Robinson, W. T. *J. Am. Chem. Soc.* **1975**, *97*, 1427–1439.
(76) Collman, J. P.; Brauman, J. I.; Doxsee, K. M.; Halbert, T. R.; Bunnenberg, E.; Linder, R. E.; LaMar, G. N.; DelGaudio, J.; Lang, G.; Spartalian, K. *J. Am. Chem. Soc.* **1980**, *102*, 4182–4192.

Table II. Effect of Solvent and Counterion on EPR Parameters for Bis(imidazole) Complexes of (TPP)FeCl[a]

complex	anion	solvent	g_1	g_2	g_3
$(TPP)Fe(Im)_2^+$	Cl^-	$CHCl_3$	2.873	2.292	1.565
	I^-	$CHCl_3$	2.866	2.294	1.562
	I^-	CH_2Cl_2	2.869	2.287	1.563
	I^-	DMF	2.898	2.288	1.565
$(TPP)Fe(4\text{-}MeIm)_2^+$	Cl^-	$CHCl_3$	2.851	2.290	1.587
	I^-	$CHCl_3$	2.849	2.280	1.605
	I^-	CH_2Cl_2	2.847	2.288	1.590
	I^-	DMF	2.869	2.276	1.587
$(TPP)Fe(N\text{-}MeIm)_2^+$	Cl^-	$CHCl_3$	2.876	2.289	1.553
	I^-	$CHCl_3$	2.879	2.295	1.546
	I^-	$CHCl_3$ + 30% EtOH	2.903	2.295	1.543
	I^-	CH_2Cl_2	2.886	2.294	1.549
	I^-	DMF	2.881	2.281	1.569

[a] g values to ±0.005.

basic than the amino or imidazole group. In cases where the exogenous ligand was less basic, 1.1 equiv of triethylamine was added for each protonated group present.

Solvents used to prepare samples for EPR experiments ($CHCl_3$, CH_2Cl_2 (Mallinckrodt SpectAR Grade), and $CDCl_3$ (Merck Sharp & Dohme)) were used as received; DMF (Aldrich Gold Label) was dried over molecular sieves (Linde 4 Å).

N-Methylimidazole, 1,2-dimethylimidazole, pyridine, and 4-methylpyridine (Aldrich) were distilled before use; imidazole, *N*-benzylimidazole, 5,6-dimethylbenzimidazole, 4-(dimethylamino)pyridine, 4-aminopyridine, 3,4-diaminopyridine (Aldrich), and 4-phenylimidazole (ICN Pharmaceuticals) were recrystallized from benzene and dried at 110 °C in vacuo before use. Pyrazoles, indazoles, triazoles, 4-methylimidazole, proton sponge, and six-membered ring heterocycles (Aldrich) and 5-chloro-*N*-methylimidazole (Sigma) were used as received. 3-Methyl-4-(dimethylamino)pyridine and 3,5-dimethyl-4-(dimethylamino)pyridine were prepared by the method of Essery and Schofield.[77]

EPR samples were prepared from stock solutions of (TPP)FeCl or (TPP)FeI and the desired ligand in the chosen solvent such that the final $[Fe^{III}]$ = 0.05 M. The Fe:ligand ratio was varied from 1:1 to as high as necessary to observe complete formation of the bis-ligand complex (often the stoichiometric 1:2). However, in the case of extremely low basicity ligands of low solubility, it was not always possible to achieve high enough ligand concentrations to completely form the bis-ligand complex. Samples were transferred to 4-mm quartz EPR tubes (Wilmad) and precooled in liquid nitrogen.

EPR spectra were recorded on a Varian E-12 spectrometer operating at X band, with 100-kHz field modulation. The magnetic field was precalibrated with an NMR gaussmeter and the frequency calibrated for each sample with the Varian weak pitch sample (g = 2.0028) or with DPPH (g = 2.0036). Spectra were typically run at ca. 100 K by using the Varian flowing nitrogen temperature controller and in some cases at 10–30 K using the Air Products flowing helium temperature controller.

Results

In Figure 3 are shown typical EPR spectra observed in this study. Observation of the high-spin signal of (TPP)Fe (trace a) was taken as evidence that the ligand did not bind or that, if it did, the product was high spin. The bis-ligand complexes of $(TPP)Fe^{III}$ with hindered imidazoles and low basicity pyridines gave no EPR signals at 77 K but below 30 K yielded the strong g_{max} ~3.4 signal (trace b) observed by Migita et al.[65] and Palmer et al.[47] for some of the same ligand complexes of protohemin. Further interpretation of this signal will be published separately.[68] The bis-ligand complexes of $(TPP)Fe^{III}$ with nonhindered imidazoles, high basicity pyridines, pyrazoles, and several other classes of heterocycles gave EPR signals similar to that shown in trace c. It is this type of EPR signal which is the subject of this paper.

In Table II are listed the EPR parameters for (TPP)FeCl and (TPP)FeI in the presence of various nonhindered imidazoles in $CHCl_3$, CH_2Cl_2, and DMF. As may be seen, the nature of the halide counterion does not affect the EPR parameters. The g values are within experimental error (±0.005) of each other in $CHCl_3$ and CH_2Cl_2, but g_z is generally larger in DMF, as it is in 70% $CHCl_3$–30% ethanol. This suggests that g_z tends to increase slightly with dielectric constant of the solvent, and thus the differences between g_z reported by Blumberg, Peisach, and Alder[14] and those reported herein for the same complexes are due to the difference in the solvent system employed.

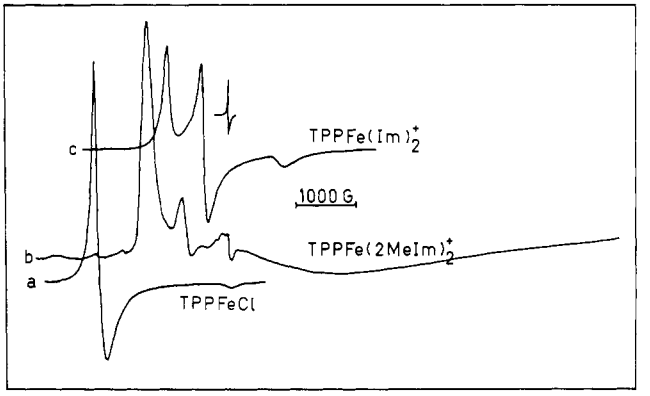

Figure 3. Typical EPR spectra observed for iron(III) porphyrins: (a) HS Fe^{III}, (b) LS Fe^{III} "strong g_{max}" or HALS signal, and (c) commonly observed rhombic LS Fe^{III} signal. The shape and intensity of the small signal components of the "strong g_{max}" signal located at ca. g = 2.4 and 2.0 vary from sample to sample and do not appear to be due to the same species as that which produces the strong g = 3.4 signal.

In Table III are listed the EPR parameters for (TPP)FeI in CH_2Cl_2 in the presence of various nitrogen bases, together with the pK_a of the conjugate acid of each base. In wet solvents a second low-spin EPR signal was often observed in the presence of imidazoles and basic pyridines which had g_z = 2.45–2.46, g_y ~ 2.1 (usually not resolved in the presence of the stronger major signal), and g_x = 1.77–1.80. These parameters are very similar to those reported for cytochrome b_2 at pH 11.5 (2.44, 2.16, 1.91),[22] metmyoglobin hydroxide (2.55, 2.17, 1.85),[14] and "signal II" of $(N\text{-}MeIm)_2$Proto(DME) in $CHCl_3$ (2.45, 2.16, 1.91).[58] All of these species have values of V/Δ and Δ/λ which lie within the "O" region of Peisach and Blumberg,[14] and they probably all represent an axial ligand combination of one imidazole and one hydroxide. In the case of the model compounds of this study and ref 58, the hydroxide ions undoubtedly come from traces of water in the solvent, deprotonated by excess axial ligand.

Although analysis of the EPR and Mössbauer spectra of the "strong g_{max}" signal of $(TPP)Fe^{III}$ with hindered imidazoles and low basicity pyridines (Figure 3b) is still in progress,[68] preliminary assignment of the second and third g values and the values of V/Δ and Δ/λ calculated therefrom are included in Table III for completeness. The assignment of g_3 follows that of Migita and Iwaizumi[65] (i.e., the center of the broad minimum between 4000 and 6000 G). However, the assignment of g_2 is made by assuming that $g_1^2 + g_2^2 + g_3^2 = 16$.[2,15,19] This is the maximum value possible if contributions to a, b, and c (eq 1, 2) from covalency can be neglected (i.e., if the orbital reduction factor k = 1).[15,16] As is apparent from the data of Table III, this assumption is met for the majority of the compexes of this study, except for the bis(pyrazole) complexes. Not only are the sums of the squares of the g values very close to 16 in the majority of cases but, also, $a^2 + b^2 + c^2 = 1.000 \pm 0.006$ for the vast majority of the com-

(77) Essery, J. M.; Schofield, K. *J. Chem. Soc.* **1960**, 4953–4959.

Table III. Effect of Axial Ligand Structure and Basicity on EPR Parameters of $(TPP)L_2^{+}$ [a]

base	$pK_a(BH^+)$ [b]	g_1	g_2	g_3	V/Δ	Δ/λ	$a^2+b^2+c^2$	$\sum g^2$
			Pyridines					
4-NMe_2Py	9.70	2.786	2.284	1.657	0.65	3.60	1.003	15.7
4-NH_2Py	9.29	2.830	2.289	1.603	0.65	3.35	1.002	15.8
3,4-$(NH_2)_2$Py	9.14	2.864	2.280	1.597	0.61	3.45	1.006	16.0
3-Me,4-NMe_2Py	8.69	2.865	2.286	1.591	0.62	3.38	1.006	16.0
3,5-Me_2,4-NMe_2Py	8.12	2.785	2.281	1.675	0.64	3.73	1.005	15.8
3,4-Me_2Py[c]	6.46	3.4	1.7(calcd)	1.2	0.15	6.53	0.997	16.0
pyridine[c]	5.20	3.4	1.7(calcd)	1.2	0.15	6.53	0.997	16.0
isoquinoline[c]	5.40	3.44	1.66(calcd)	1.19	0.14	7.07	1.000	16.0
			Pyrazines					
pyrazine[d]	0.65							
2-MePyrz[d]	1.45							
			Pyrimidines					
pyrimidine[d]	1.98							
quinazoline[d]	3.51	2.781	2.277	1.687	0.63	3.84	1.006	15.8
			Pyridazines					
pyridazine[d]	2.33							
3-MePydz[d]	~3.0[e]	2.862	2.24(calcd)	1.655	0.53	4.13	1.009	16.0
cinnoline[d]	2.42							
phthalazine[d]	3.47	2.801	2.200	1.734	0.47	5.15	1.009	15.7
			Triazines					
s-triazine	~1.4[e]	2.747	2.284	1.646	0.70	3.43	0.995	15.5
1,2,4-benzotriazine[d]								
			Imidazoles					
N-MeIm	7.33	2.886	2.294	1.549	0.64	3.17	1.004	16.0
4-MeIm	7.22[f]	2.847	2.288	1.590	0.64	3.32	1.003	15.9
N-Bzlim	~7.0[e]	2.860	2.306	1.561	0.67	3.10	1.003	15.9
imidazole	6.65[f]	2.869	2.287	1.563	0.63	3.24	1.002	15.9
4-PhIm	5.70[f]	2.893	2.307	1.552	0.65	3.12	1.008	16.1
5-Cl,*N*-MeIm	4.75[g]	2.884	2.308	1.533	0.66	3.02	1.004	16.0
2-MeIm[c]	7.56[f]	3.399	1.74(calcd)	1.188	0.17	5.88	1.000	16.0
5,6-Me_2-bzlIm[c]	5.68[f]	3.432	1.67(calcd)	1.194	0.14	6.96	1.000	16.0
1,2-Me_2Im[c]	7.85	3.400	1.67(calcd)	1.289	0.12	8.65	1.002	16.0
			Pyrazoles and Indazoles					
3-NH_2Pz 1:1	~5.5[e,f]	2.407	2.294	1.845	1.27	3.52	0.990	14.5
3-NH_2Pz 1:10	~5.5[e,f]	2.389	2.284	1.861	1.28	3.68	0.991	14.4
5-NH_2Iz[c]	4.9[f]	3.61						
6-NH_2Iz	3.7[f]	2.532	2.363	1.771	1.19	2.91	0.996	15.1
3-MePz	3.3[f]	2.581	2.382	1.739	1.15	2.78	0.999	15.4
4-IPz	2.7[e,f]	2.599	2.389	1.703	1.15	2.63	0.995	15.4
pyrazole	2.2[f]	2.615	2.378	1.714	1.07	2.79	0.998	15.4
indazole	1.0[f]	2.679	2.397	1.630	1.04	2.51	0.995	15.6
3,5-Me_2Pz[c,d]		2.609						
			Triazoles					
3-NH_2,1,2,4-Tz	3.74[f]	2.493	2.337	1.795	1.20	3.11	0.993	14.9
		2.597	2.335	1.735	0.97	3.15	0.994	15.2
		2.635	2.337	1.735	0.91	3.25	1.000	15.4
1,2,4-Triazole 1:2	1.97[f]	2.983	2.323	1.374	0.67	2.55	1.006	16.2
1,2,4-triazole 1:5		2.979	2.298	1.429	0.62	2.82	1.007	16.2
s-triazole[4,3-*a*]quinoline	~1.3[e]	2.901	2.342	1.449(calcd)	0.73	2.58	1.001	16.0
benzotriazole[c]	1.3[f]	2.592						

[a] Solvent = CH_2Cl_2; *g* values to ±0.005. [b] References 78 or 79 unless otherwise indicated. [c] No signal at 77 K; strong $g \sim 3.4$ signal at <30 K. [d] Large HS Fe^{III} signal (g = 6,2) observed at 77 K. [e] Estimated from Figure 4. [f] Corrected for the presence of two H^+ (0.3). [g] Gallo, G. G.; Pasqualucci, C. R.; Radaelli, P.; Lancini, G. C. *J. Org. Chem.* **1964**, *29*, 862–865.

plexes of this study (Table III), including the pyrazole complexes and the "large g_{max}" species whose g_2 and g_3 values have been assigned as described above. The complexes of this study (Table III) follow the $g_1^2 + g_2^2 + g_3^2 = 16$ and $a^2 + b^2 + c^2 = 1$ criteria[2,15,19] much better than those reported previously (Table I), especially those reported for the heme proteins. Such calculation of g_2 for the "strong g_{max}" signal (Figure 3, Table III) yields values of ca. 1.7, rather than the values of ca. 2.4 reported by Migita and Iwaizumi.[65] We find that the signal at $g \sim 2.4$ varies in intensity relative to the "strong g_{max}" signal as a function of sample preparation and is thus probably due to an impurity.

Discussion

Effect of the Structure and Basicity of the Axial Ligand on the EPR Parameters of $(TPP)FeL_2^+$. In an attempt to shed light on the effect of the electronic properties of the imidazole ligand on the magnetic properties of ferriheme proteins, several previous studies of the relationship between axial ligand basicity and EPR parameters of low-spin bis-ligand ferric porphyrin complexes have been carried out.[14,54] One of these studies, which has been widely quoted, suggested that the *g* values approach each other as the axial ligands become less basic.[54] However, different classes of ligands (imidazoles, pyridines, pyrazoles, triazoles, etc.) were included in the data used to arrive at this conclusion.[54] Our own initial studies suggested that the EPR parameters might depend not only upon ligand basicity but also upon ligand type (Figure 2), and we thus undertook an extensive study of the relationship between ligand basicity within each structural type of Figure 2 and the EPR parameters of the low-spin complexes $(TPP)FeL_2^+$. The results of this study are summarized in Table III and Figure 4, where the *g* values observed are plotted against the basicity of

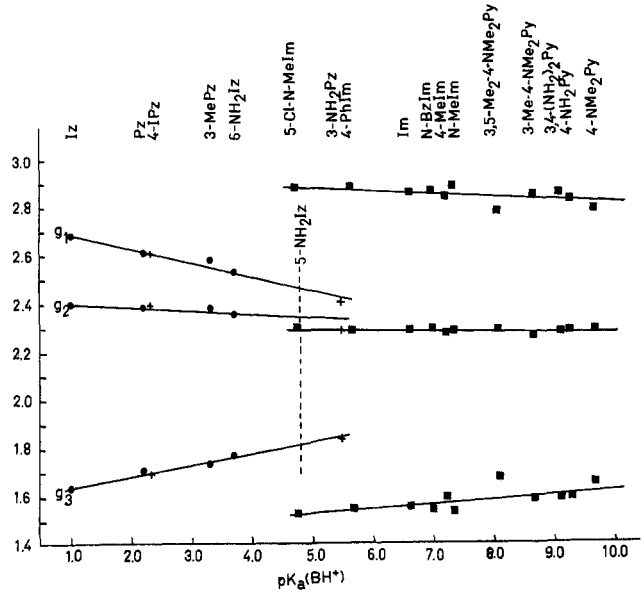

Figure 4. Variation of the g value of commonly observed rhombic LS Fe^{III} complexes (Figure 3c) with basicity of the axial ligand for pyrazoles (Pz) and indazoles (Iz), imidazoles (Im), and pyridines (Py). For calculation of rhombicity and tetragonality, g_1, g_2, and g_3 have been defined as g_z, g_y, and g_x, respectively.

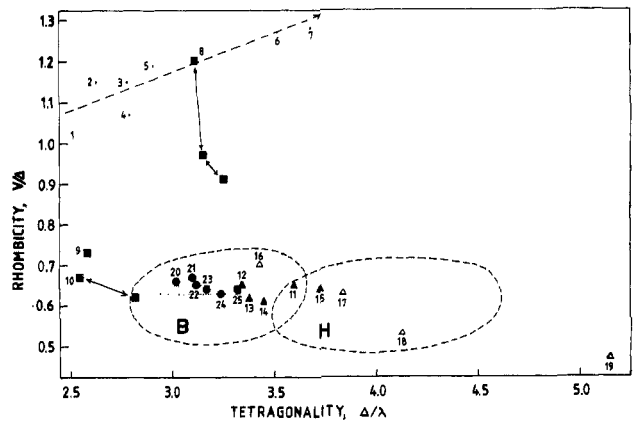

Figure 5. Plot of rhombicity (V/Δ) vs. tetragonality (Δ/λ) for the majority of low-spin Fe^{III} TPP complexes of this study. The areas B and H are those defined by Blumberg and Peisach (Figure 1b), as defined by the heme proteins of Table I. Ligands are as follows: (1) Iz; (2) 4-IPz; (3) 3-MePz; (4) Pz; (5) 6-NH_2Iz; (6) 3-NH_2Pz, 1:1 ratio; (7) 3-NH_2Pz, 1:10 ratio; (8) 3-NH_2, 1,2,4-Tz; (9) 5-Triazolo[3,4-*a*]quinoline; (10) 1,2,4-Tz; (11) 4-NMe_2Py; (12) 4-NH_2Py; (13) 3-Me, 4 NMe_2Py; (14) 3,4$(NH_2)_2$Py; (15) 3,5-Me_2,4-NMe_2Py; (16) Trz; (17) quinazoline; (18) 3-MePdz; (19) phthalazine; (20) 5-Cl,NMeIm; (21) *N*-BzlIm; (22) 4-PhImH; (23) NMeIm; (24) ImH; (25) 4-MeImH. The line through the pyrazole/indazole data shows the approximately linear relationship of rhombicity and tetragonality, and the arrow shows the direction of increasing nitrogen basicity toward the proton. The two signals observed with 1,2,4-triazole and the three with 3-amino-1,2,4-triazole as ligands are connected by double-pointed arrows, but no structural assignment of these species is given. The dotted rectangular area shows the extent of variation in rhombicity and tetragonality of meta- and para-substituted (TPP)Fe(*N*-MeIm)$_2^+$ complexes (Table IV).

the axial ligand for each of the three major types: pyridines, imidazoles, and pyrazoles.

There is a large gap in the basicity of commercially available nonsterically hindered pyridines (3,4-dimethylpyridine, $pK_a(BH^+)$ = 6.46,[78] and 4-aminopyridine, $pK_a(BH^+)$ = 9.29[79]). The lower basicity pyridine complexes with (TPP)FeI do not give resolved EPR spectra at liquid nitrogen temperature, but rather give the strong g = 3.4 signal shown in Figure 3b at temperatures below 30 K, as reported previously for the same complexes of protohemin.[65,47] We therefore prepared several 4-(dimethylamino)-pyridines in which the amino group is sterically prevented from being in full conjugation with the aromatic ring,[71] thereby lowering the basicity of the aminopyridine (Table III). All of the aminopyridines investigated ($pK_a(BH^+)$ = 8.12–9.70[79]) formed complexes with well-resolved EPR signals at ca. 100 K of the type shown in Figure 3c. Thus, the minimum pyridine basicity necessary to produce a resolved "B hemichrome"-type EPR signal is less than 8.12 but greater than 6.46. Synthesis of additional non-2,6-substituted pyridines whose conjugate acids have pK_a values between these two values would allow further study of the factors affecting the change in EPR signal from that of Figure 3b to that of Figure 3c. This subject will be addressed further in a later study.[68]

In contrast to pyridine ($pK_a(BH^+)$ = 5.20[78]), pyridazine ($pK_a(BH^+)$ = 2.33[78]) forms a bis-ligand complex with (TPP)FeI which gives a resolved low-spin EPR spectrum; pyrazines and pyrimidines, however, do not. Thus, it appears that the existence or lack thereof of a low-spin EPR signal of bis six-membered ring heterocycle complexes of (TPP)FeI depends not only upon ligand basicity but also upon ligand type. That this is the case becomes all the more clear when one looks at the EPR parameters of bis(azole) complexes of (TPP)FeI: imidazole ligands ranging in basicity from $pK_a(BH^+)$ = 4.47–7.33[77,78] produce low-spin ferric porphyrin complexes with almost identical EPR parameters (Table III, Figure 4), while pyrazole and indazole complexes in which the ligands range in basicity[77,78] from $pK_a(BH^+)$ = 1.0 to ca. 5.5 have a much smaller spread in g values than the bis(imidazole) complexes, a spread which becomes smaller as $pK_a(BH^+)$ increases (Figure 4)—the opposite trend from that reported previously.[54]

Triazoles produce complexes which range from a slightly greater to considerably smaller spread in g values than imidazoles and aminopyridines.

The data of Table III are graphically summarized in Figure 4, where lines have been drawn to illustrate the variation or lack thereof in g_x, g_y, and g_z with the basicity of each type of axial ligand. As may be seen, all basic pyridines and nonhindered imidazoles appear to be grouped together; they all have very similar EPR parameters, with only a slight trend toward convergence of the three g values with increasing basicity. In contrast, the EPR parameters of pyrazole and indazole complexes converge strongly as a function of ligand basicity, and at the point of approximate overlap in basicity (4-phenylimidazole vs. 3-aminopyrazole), the bis(pyrazole) complex has a nearly axial ($g_z \approx g_y \neq g_x$ in the axis system used for imidazoles) EPR spectrum while the bis(imidazole) complex is typically rhombic (Figures 3c, 4).

As another means of illustrating the basic difference between imidazoles and other azoles, the rhombicity (V/Δ) vs. tetragonality (Δ/λ) of the complexes is plotted in Figure 5. As expected, all bis(imidazole) and most bis(aminopyridine) complexes lie very close together within the B region defined by Peisach and Blumberg for the complexes of Table I, while one of the bis(aminopyridine) complexes lies somewhat within the H region. Photoelectron spectra of 4-NMe_2Py and 4-NH_2Py have been reported[80] and are unique among substitued pyridine spectra, in that the ionization potential for π_s, the π orbital with large amplitude at nitrogen, is considerably less than that for the n (σ) orbital on nitrogen: For 4-NMe_2Py ($pK_a(BH^+)$ = 9.70[78]), π_s lies ca. 1.2 eV higher in energy than n; for 4-NH_2Py ($pK_a(BH^+)$ = 9.29[79]), the difference is much smaller—π_s lies ca. 0.4 eV higher in energy than n. Photoelectron spectra of the other aminopyridines of this study have not been reported. However, the next most basic pyridine whose ionization potentials have been reported, 2,4,6-Me_3Py ($pK_a(BH^+)$ = 7.48[81]), has π_s lower than n by 0.4 eV.[80]

(78) Albert, A. In "Physical Methods in Heterocyclic Chemistry"; Katritzky, A. R., Ed.; Academic Press: New York, 1963; Vol. I, pp 1–108.
(79) Albert, A. In "Physical Methods in Heterocyclic Chemistry"; Katritzky, A. R., Ed.; Academic Press: New York, 1971; Vol. III, pp 1–26.
(80) Ramsey, B. G.; Walker, F. A. *J. Am. Chem. Soc.* **1974**, *96*, 3314–3316.
(81) Jencks, W. P.; Regenstein, J. In "Handbook of Biochemistry and Molecular Biology"; Fasman, G. D., Ed.; CRC Press: Cleveland, 1977; p 339.

In comparison, all imidazoles whose ionization potentials have been reported have n and π orbitals of nearly identical energy.[82] Thus, those pyridines which have EPR parameters, rhombicities, and tetragonalities similar to those of imidazoles have in common with the imidazoles the potential for π-donor interactions with the Fe^{III} porphyrin. Similar consideration of π-donor as compared to σ-donor ability has recently been applied to the variation (or lack thereof) in quadrupole splitting constants of a series of pentacyanoiron(III) pyridine and azole complexes.[83] This variation in σ-donor vs. π-donor properties may also contribute to the change in the type of low-spin EPR signal observed for low basicity pyridines, discussed above (Table III, Figure 3b), since π_3 is significantly lower in energy than n for all low basicity pyridines.[80]

It is worth pointing out, in fact, that the most common ligands bound to the axial positions of iron in heme proteins are fairly strong π donors: imidazole, imidazolate, thio ether, mercaptide, hydroxide, and even dioxygen, but not the physiological poisons carbon monoxide and cyanide. The first five ligands mentioned, and their combinations, form the basis of the correlation system of Blumberg and Peisach[12,14] (Figure 1, bottom). Since LS Fe^{III} lacks an electron in the d_π orbitals, L $\rightarrow$ M π donation can occur from the axial ligands to Fe^{III}. Evidence for this π-electron donation has been obtained from NMR studies of axial ligands bound to LS iron(III) porphyrins[84] and from Mössbauer studies of pentacyanoiron(III)–ligand complexes.[83] Such L $\rightarrow$ M π donation could not occur in the reduced (Fe^{II}) forms of these proteins, since the d_π orbitals are filled. Thus, the π-donor character of the axial ligands of common heme proteins may play an important role in the redox, oxygenation, and oxidase properties of these proteins. Aliphatic amines, earlier proposed as axial ligands for several forms of cytochromes *c*,[39] have no potential π-acceptor or π-donor properties.

Pyrazoles and indazoles define a new group in which the rhombicity is much greater than two-thirds, indicating a change in magnetic axes.[21] In the case of this group of ligands, tetragonality increases strongly as the basicity of the ligand increases, as expected from the definition of Δ/λ.[9,19,21]

Among azoles in general there are several tautomeric forms possible unless an alkyl group is bound to the nitrogen. It is assumed throughout this work that the nonsterically hindered tautomer is that which binds to the iron porphyrin. Evidence in support of this assumption includes the following:

(1) The equilibrium constant (β_2) for bisligand complex formation of 4(5)-methylimidazole with (TPP)FeCl is very similar to that of imidazole and quite different from that of 2-methylimidazole.[85]

(2) The EPR spectra of the bis-ligand complexes of 4(5)-methylimidazole and 4(5)-phenylimidazole are very similar to other nonhindered imidazoles (Figure 3c) rather than to that of 2-methylimidazole (Figure 3b).

(3) 3(5)-methyl- and 3(5)-aminopyrazole form low-spin bisligand complexes with (TPP)Fe^{III} which give well-resolved EPR spectra at the liquid nitrogen temperature (Table III), whereas addition of 3,5-dimethylpyrazole to a solution of (TPP)FeI produces an EPR signal only below 30 K similar to that of Figure 3b, except that the strong signal is at $g = 2.61$.

(4) The [tetrakis(3-methylpyrazole)]manganese(II) bromide complex has been shown by X-ray crystallography to have the ligand bound as the 5-methylpyrazole tautomer.[86]

(5) The evidence for indazole binding to metals through the "pyridine" nitrogen, N_2, has been summarized.[87]

Thus, the actual basicity of the azole ligand in the tautomer which binds in the cases of 4(5)-methylimidazole, 4(5)-phenylimidazole, 3(5)-methylpyrazole, 3(5)-aminopyrazole, and 1,2,4-triazole and its 3-amino derivative may be somewhat different from those measured by aqueous pH titration. All pK_a values for the conjugate acids of azoles (except N-substituted azoles) have been corrected for the statistical factor (log 2) which is due to the fact that in principle, at least, either proton might be lost on acid dissociation.

The behavior of 5- and 6-aminoindazole requires some additional discussion The 5-substituted isomer is the more basic ($pK_a(BH^+) = 5.15$[78] or 5.27[88]), but it does not form a complex with (TPP)FeI which produces a resolved EPR signal at either 100 K or below 30 K, whereas 6-aminoindazole forms a bis-ligand complex which produces a well-resolved pyrazole-type (Figure 4) EPR signal at 100 K. The reason for the anomalous behavior of 5-aminoindazole has recently been explained in part by a study of the absorption and fluorescence spectra of this compound as a function of pH,[88] which has shown that in the ground electronic state, protonation occurs on the amino nitrogen rather than the pyrazole "pyridine" nitrogen. Thus, protonation of the two aminoindazoles occurs quite differently due to the resonance stabilization present in the 6-amino but not the 5-amino isomer:

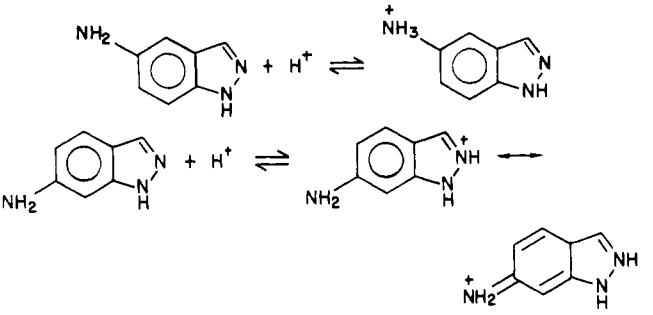

Thus, the 5-amino isomer is a much poorer electron-pair donor toward the proton and, thus, not surprisingly, toward transition metals. Added to this difference is the insolubility of 5-aminoindazole, which precludes achieving ligand concentrations similar to those used for indazole complex formation with (TPP)FeI (0.5 M). Such high ligand concentrations were not required for 6-aminoindazole, which complexes more readily than indazole to (TPP)FeI because of the greater basicity of its "pyridine" nitrogen.

Triazoles of the 1,2,4 type have two possible tautomers which may bind to (TPP)FeCl or three if a 3-amino substituent is present:

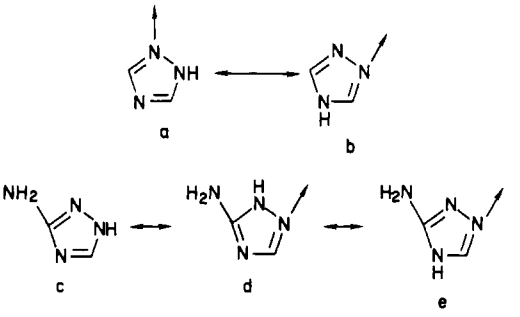

In addition to these tautomeric forms, there are a number of possible zwitterionic forms possibly involving the amino group. Of these only f is capable of coordinating to Fe^{III} if the same arguments involving coordination of the nonhindered form of the ligand as discussed above are invoked, while d and e can coordinate only through the nitrogen indicated by the arrow, and c cannot coordinate. As for a and b, a has two different nitrogen coor-

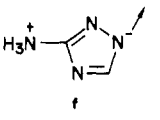

(82) Ramsey, B. G. *J. Org. Chem.* **1979**, *44*, 2093–2097.
(83) Johnson, C. R.; Shepherd, R. E. *Inorg. Chem.* **1983**, *22*, 3506–3513.
(84) Chacko, V. P.; LaMar, G.N. *J. Am. Chem. Soc.* **1982**, *104*, 7002–7007.
(85) Walker, F. A.; Lo, M.-W.; Ree, M. T. *J. Am. Chem. Soc.* **1976**, *98*, 5552–5560.
(86) Reedijk, J.; Stork-Blaisse, B. A.; Verschoor, G. C. *Inorg. Chem.* **1971**, *10*, 2594–2599.
(87) Reedijk. *J. Transition Met. Chem.* **1979**, *4*, 335.
(88) Swaminathan, M.; Dogra, S. K. *J. Am. Chem. Soc.* **1983**, *105*, 6223–6228.

dination sites, while in b the two "pyridine" nitrogens are equivalent. The EPR spectrum of (TPP)FeI in the presence of 1,2,4-triazole contains two low-spin signals whose ratios vary as the amount of ligand is increased, while that of (TPP)FeI in the presence of 3-amino-1,2,4-triazole contains three low-spin species whose ratios do not change with ligand concentration. The EPR parameters of all of these species are listed in Table III and shown in Figure 5, but assignment of the signals to particular ligand coordination modes would involve pure speculation. *s*-Triazolo-[3,4-*a*]quinoline (see Figure 2) is a 1,2,3-triazole which can coordinate only through the middle nitrogen due to steric considerations. It forms only one complex with (TPP)FeI. In contrast, benzotriazole, also a 1,2,3-triazole, does not form a typical (Figure 3c) low-spin complex with (TPP)FeI, though the basicities of the two ligands are probably similar. The reason for this difference in behavior is not clear.

In aqueous solution, monocomplex formation constants between metal ions and pyrazole as compared to imidazole are ca. 2 orders of magnitude smaller when the metal is Cu^{2+} and 1 order of magnitude smaller when it is Ni^{2+} or Zn^{2+},[89] while the pK_a values for the conjugate acids of pyrazole and imidazole differ by nearly 4 pK units[78] (Table III). Such comparisons have led previous workers to question why pyrazoles are better bases toward metal ions than they are toward the proton. The answer appears to involve two concepts: (1) "unexpectedly" low proton affinity of pyrazole relative to imidazole due to extra destabilization of the π bonding of the former compound after protonation[90] and (2) the fact that pyrazoles are better π donors than imidazoles because the valence π orbital of pyrazole has large amplitude at the "pyridine" nitrogen, while that of imidazole has small amplitude at that nitrogen.[90,91] In the present case of the metal being (TPP)Fe^{III}, the formation constant (β_2) of the bis(pyrazole) complex of (TPP)FeCl in $CHCl_3$ at 25 °C was too small to be measured (<1 M^{-2}) by ligand titrations using cyclic voltammetric techniques.[92] This is at least 6 orders of magnitude smaller than that for bis(imidazole) complex formation in the same solvent.[85] While this is a larger decrease in stability than observed in the aqueous complex formation studies,[89] two ligands are involved rather than one. However, the $\beta_2 < 1$ M^{-2} estimate is at least 2 orders of magnitude smaller than what would be expected for an imidazole of the same pK_a(BH^+), based upon the values of β_2 measured previously for substituted imidazoles binding to (TPP)FeCl.[85] Nevertheless, at the low temperatures used for EPR measurements, the pyrazole complexes were sufficiently stable that complete formation occurred with most ligands (except indazole) when only slightly greater than a 2:1 ratio of ligand to (TPP)FeI was present.

Pyrazoles, imidazoles, triazoles, and aminopyridines all have similar ranges of the tetragonality parameter, Δ/λ, indicated by Figure 5 and Table III. Thus, they all provide approximately the same axial ligand field, as sensed by the iron orbitals. However, the geometries of the pyrazole complexes, as measured by the rhombicity parameter, V/Δ, differ considerably from those of the others. Though the direction of g_z is usually taken to be normal to the heme plane,[19] without knowing the orientation of the g tensors with respect to the molecular axes, it is not possible to state with certainty the nature of the difference in the magnetic axes of the majority and of the pyrazole complexes.

Effect of Porphyrin Substituents on the EPR Parameters of (TPP)Fe(*N*-MeIm)$_2^+$Cl$^-$. We have recently studied the effect of symmetrical and unsymmetrical phenyl substitution on the NMR spectra of a series of bis(*N*-methylimidazole) complexes of (TPP)Fe^{III}.[93] It was found that the pyrrole proton isotropic shift varies slightly with the electron-donating or withdrawing nature of the phenyl substituents, as measured by the sum of their Hammett σ constants, with larger (further upfield) isotropic shifts being found when $\sum\sigma$ is positive than when it is negative. More important, unsymmetrically phenyl-substituted (TPP)Fe(*N*-MeIm)$_2^+$ complexes showed a splitting of the pyrrole proton resonance into two to four peaks, depending on the symmetry of the substitution pattern and the nature of the substituents.[93] We were therefore interested to see how the EPR parameters would vary as a function of $\sum\sigma$ and unsymmetrical substitution pattern. Thus, EPR spectra were recorded of all of the NMR samples in $CDCl_3$. The results are tabulated in Table IV. It is evident that there is a small tendency toward convergence of g_x, g_y, and g_z as $\sum\sigma$ increases, but there is no indication that unsymmetrical phenyl subsitution affects the g anisotropy. The effect of the variation in the EPR parameters with $\sum\sigma$ upon Δ/λ and V/α is extremely small: all of the species of Table IV lie within a small rectangular area of Figure 5, with the average $V/\Delta = 0.64 \pm 0.01$ and Δ/λ ranging from 2.97 for electron-donating substituents to 3.33 for electron-withdrawing groups. This is the opposite trend from that expected for axial ligands.[9,19,21] As is evident from the rectangular area designated in Figure 5, porphyrin substituents have a small effect upon the total charge felt by the iron.

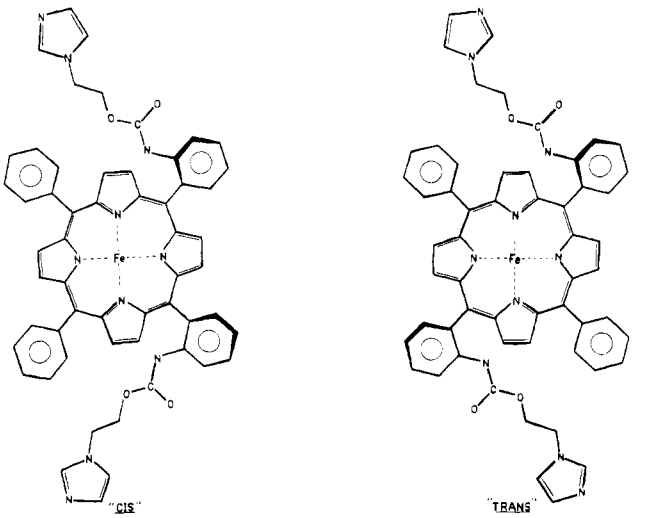

Figure 6. Structures of the 6-coordinate porphyrins prepared for this study, abbreviated as ((Im$CH_2CH_2OCONH)_2$TPP)Fe^{III}: The "cis" isomer was expected to hold the axial ligands in perpendicular and the "trans" in parallel planes.

Effect of Covalent Attachment of Axial Ligands and Axial Ligand Plane Orientation on the EPR Parameters of Low-Spin Iron(III) Porphyrins. It was originally hoped that covalent attachment of axial ligands through *o*-phenyl side arms would lead to cytochrome *b* models in which the axial ligands were required to be either mutually parallel, as in the so-called "trans" isomer of Figure 6, or mutually perpendicular, as in the "cis" isomer of Figure 6. In order for these geometries to be maintained, each axial imidazole plane must lie over the meso position to which its phenyl ring is attached. Though CPK molecular models suggest that this should be the case for the "cis" and "trans" isomers of Figure 6, the results of the molecular structure determinations of a 5-coordinate zinc side-arm porphyrin[94] and a monoimidazole side-arm iron porphyrin containing a thio ether as the sixth ligand[95] both suggested that the axial ligands of Figure 6 would be able to rotate at least 45° from the desired plane orientation over the meso positions. Thus, both the cis and trans isomers of Figure 6 may contain an equimolar mixture of parallel and perpendicular orientations of their axial ligand planes. In Table V are listed the EPR parameters of the two isomers and related complexes to be discussed below. Interestingly, both isomers show identical EPR spectra which consist of approximately equal height signals from high-spin Fe(III) and the low-spin bis(imidazole) complex.

(89) Aruga, R. *J. Inorg. Nucl. Chem.* **1981**, *43*, 2459–2461.
(90) Olivella, S.; Vilarrasa, J. *J. Heterocycl. Chem.* **1981**, *18*, 1189–1196.
(91) Bernarducci, E.; Schwindinger, W. F.; Hughey, J. L.; Krogh-Jespersen, K.; Schugar, H. J. *J. Am. Chem. Soc.* **1981**, *103*, 1686–1691.
(92) Wu, M. Z. M.S. Thesis, San Francisco State University, 1979.
(93) Walker, F. A.; Balke, V. L.; McDermott, G. A. *J. Am. Chem. Soc.* **1982**, *102*, 1569–1574.
(94) Bobrik, M. A.; Walker, F. A. *Inorg. Chem.* **1980**, *19*, 3383–3390.
(95) Mashiko, T.; Marchon, J.-C.; Musser, D. T.; Reed, C. A.; Kastner, M. E.; Scheidt, W. R. *J. Am. Chem. Soc.* **1979**, *101*, 3653–3655.

Table IV. Effect of Phenyl Substituents on the EPR Parameters of Bis(*N*-methylimidazole) Complexes of (Tetraphenylporphrin)iron(III)[a]

substituents	$\sum\sigma^b$	g_z	g_y	g_x	V/Δ	Δ/λ
1 *m*-F, 3 *m*-NO_2	2.467	2.825	2.294	1.607	0.66	3.33
1 *m*-CH_3, 3 *m*-NO_2	2.061	2.835	2.288	1.592	0.65	3.31
4 *p*-COOEt	1.800	2.881	2.289	1.575	0.62	3.31
1 *m*-NO_2, 3 *m*-F	1.721	2.846	2.291	1.579	0.65	3.25
4 *m*-Cl	1.492	2.886	2.283	1.552	0.62	3.24
4 *p*-$CONMe_2$	1.440	2.867	2.289	1.560	0.64	3.21
4 *p*-$CONHCH_2CH_2CH_2CH_3$	1.440	2.876	2.289	1.558	0.63	3.22
4 *m*-F	1.348	2.852	2.274	1.562	0.63	3.28
4 *p*-Cl	0.908	2.861	2.285	1.556	0.64	3.20
1 *p*-NO_2	0.778	2.861	2.282	1.556	0.64	3.22
1 *m*-NO_2	0.710	2.856	2.289	1.566	0.65	3.22
1 *m*-NO_2, 3 *m*-CH_3	0.503	2.855	2.290	1.561	0.65	3.18
1 *p*-OCH_3, 3 *p*-Cl	0.413	2.874	2.281	1.540	0.63	3.17
1 *p*-NO_2, 3 *p*-CH_3	0.268	2.876	2.281	1.540	0.63	3.18
1 *m*-$NHCOCH_3$	0.21	2.871	2.29	1.549	0.64	3.16
1 *m*-OCH_3	0.115	2.876	2.283	1.535	0.64	3.14
1 *p*-NEt_2, 3 *p*-Cl	0.081[c]	2.876	2.279	1.535	0.63	3.16
4 H	0	2.876	2.289	1.533	0.65	3.10
1 *p*-$NHCOCH_3$	−0.01	2.865	2.287	1.554	0.64	3.19
1 *p*-OCH_3, 3 *p*-F	−0.082	2.878	2.287	1.547	0.63	3.18
1 *p*-CN, 3 *p*-OCH_3	−0.144	2.860	2.286	1.553	0.65	3.18
1 *p*-OCH_3	−0.268	2.872	2.284	1.543	0.64	3.17
4 *m*-CH_3	−0.276	2.879	2.285	1.533	0.64	3.13
1 *p*-Cl, 3 *p*-OCH_3	−0.577	2.882	2.288	1.544	0.63	3.17
1 *p*-NH_2	−0.66	2.877	2.287	1.522	0.65	3.06
4 *p*-CH_3	−0.680	2.875	2.284	1.533	0.64	3.13
2 *p*-NEt_2, 2 *p*-Cl, trans	−0.746[c]	2.876	2.282	1.527	0.64	3.11
2 *p*-NEt_2, 2 *p*-Cl, cis	−0.746[c]	2.878	2.282	1.521	0.64	3.09
4 *p*-OCH_3	−1.072	2.871	2.282	1.542	0.64	3.17
1 *p*-Cl, 3 *p*-NEt_2	−1.573[c]	2.880	2.282	1.516	0.64	3.07
4 *p*-NEt_2	−2.40	2.898	2.301	1.508	0.65	2.97

[a] Spectra measured in $CDCl_3$; *g* values to ±0.005. [b] Taken from: Swain, C. G.; Lupton, E. C. *J. Am. Chem. Soc.* **1968**, *90*, 4328–4337. Hansch, C.; Leo, A.; Unger, S. H.; Kim, K. H., Nikaitani, D.; Lien, E. J. *J. Med. Chem.*, **1973**, *16*, 1207–1216. [c] Calculated by assuming $\sigma(NEt_2) = -0.60$. McDermott, G. A.; Walter, F. A. *Inorg. Chim. Acta* **1984**, *91*, 95–102. Balke, V. L.; Walker, F. A. submitted for publication in *Inorg. Chim. Acta*.

Table V. EPR Parameters of Covalently Attached or Sterically Crowded Bis(alkylimidazole) Derivatives of $(TPP)Fe^{III}$

complex	added L	g_z	g_y	g_x	V/Δ	Δ/λ
trans-$((ImCH_2CH_2OCONH)_2TPP)FeCl$		2.859	2.297	1.564	0.66	3.17
cis-$((ImCH_2CH_2OCONH)_2TPP)FeCl$		2.860	2.311	1.547	0.68	3.01
$((o\text{-}NHCOC(CH_3)_3)_4TPP)FeCl$ (mixture of isomers)	NMeIm	2.899	2.280	1.548	0.61	3.27

[a] *g* values to ±0.005; solvent = $CDCl_3$.

The spectra of the low-spin species are, however, broader than that of $(TPP)Fe(N\text{-}MeIm)_2^+Cl^-$. The existence of the high-spin Fe(III) signals in each sample may indicate rotation of the amino groups from their desired "up–down" relationship during insertion of iron, as we have observed for atropisomers of the "picket fence" porphyrin[95] and/or intermolecular sharing of ligand arms as observed for a covalently attached imidazole derivative of the picket fence.[76] Because of the behavior of the mono covalently attached imidazole (TPP)Fe complex to be described below, we doubt that the bis covalently attached imidazole complexes of Figure 6 would engage in intermolecular sharing of ligand arms unless the two ligand arms were on the same side of the porphyrin plane. Such intermolecular sharing could lead to broadening of the EPR signal, as could the presence of two rotational geometries.

We recently reported an NMR study of the restricted axial ligand rotation of *N*-methylimidazole when bound to the $\alpha\alpha\beta\beta$, $\alpha\beta\alpha\beta$, and $\alpha\alpha\alpha\beta$ atropisomers of (tetrakis(*o*-pivalamidophenyl)porphinato)iron(III),[96] where α and β refer to the orientation "up" and "down" of the *o*-pivalamido substituents with respect to the plane of the porphyrin ring. In that work we found that it was not possible to separate the atropisomers from one another, but nevertheless it was possible to show that the $\alpha\alpha\beta\beta$ atropisomer had its axial ligands in the same plane (on the average) while the $\alpha\beta\alpha\beta$ atropisomer had its axial ligands in perpendicular planes. However, the samples were contaminated with nearly 50% of the $\alpha\alpha\alpha\beta$ atropisomer, due to phenyl ring rotation during insertion of iron.[96] The relative planar orientation of the two axial ligands in the $\alpha\alpha\alpha\beta$ atropisomer is difficult to predict and may actually be variable. Thus, it is not surprising that all samples of tetrakis(*o*-pivalamidophenyl)porphinatoiron(III) bis(*N*-methylimidazole) prepared for the NMR study[96] gave EPR spectra essentially identical with that of $(TPP)Fe(N\text{-}MeIm)_2^+$ in $CDCl_3$. Thus, this system provides no information concerning the effect of axial ligand plane orientation on *g* values and magnetic anisotropy. Additional sterically crowded (TPP)Fe(III) derivatives are being prepared in an attempt to separate the isomers and allow the EPR spectra of each isomer to be observed.

Properties of Mixed-Ligand Complexes of the Five-Coordinate Porphyrin (o-$ImCH_2CH_2OCONHTPP$)FeCl. The monoalkylimidazole side-arm porphyrin prepared for this study provided the opportunity to investigate the EPR parameters of mixed-ligand Fe(III) porphyrin complexes, $(ImCH_2CH_2OCONHTPP)FeL^+Cl^-$, which would be difficult to investigate in the absence of covalent attachment of the imidazole, particularly in those cases where L is a weaker ligand than the imidazole. Table VI lists the EPR parameters of a number of mixed-ligand complexes. One type of mixed ligand complex presented in Table VI is that involving one covalently attached alkylimidazole ligand and one deprotonated or hydrogen-bonded exogenous imidazole and, for completeness, the bis-deprotonated or hydrogen-bonded imidazole complex produced by adding an excess of exogenous imidazole and a deprotonating agent. While this work was in progress, Quinn, Nappa, and Valentine published a detailed study of the

(96) Walker, F. A.; Buehler, J.; West, J. T.; Hinds, J. L. *J. Am. Chem. Soc.* **1983**, *105*, 6923–6929.
(97) DelGaudio, J.; LaMar, G. N. *J. Am. Chem. Soc.* **1978**, *100*, 1112–1119.

Table VI. EPR Parameters of Mixed-Ligand Complexes of the 5-Coordinate Porphyrin ($ImCH_2CH_2OCONH$) (TPP)FeCl[a]

L_1	L_2	g_z	g_y	g_x	V/Δ	Δ/λ
RIm[b]	NMeIm	2.874	2.292	1.563	0.644	3.22
RIm[b]	ImH[c]	2.873	2.297	1.560	0.65	3.17
ImH[c,d]	ImH[c]	2.863	2.293	1.562	0.65	3.19
RIm[b]	$ImH\cdots NEt_3$[e]	2.850	2.289	1.593	0.64	3.34
RIm[b]	Im^-[f]	2.857	2.289	1.584	0.64	3.31
$ImH\cdots Et_3N$[g]	$ImH\cdots Et_3N$[g]	2.779	2.274	1.682	0.63	3.82
RIm[b]	pz	2.647	2.307	1.753	0.80	3.66
RIm[b]	$3\text{-}NH_2Pz$	2.826	2.290	1.662	0.62	3.68
RIm[b]	1,2,4-triazole	2.814	2.292	1.665	0.64	3.65
RIm[b]	2-MeIm	3.262	2.050	1.076[h]	0.38	2.98
RIm[b]	3,4-lutidine	3.284	*i*	*i*		

[a] g values to ±0.005; solvent = CH_2Cl_2. [b] The side arm, $ImCH_2CH_2OCONH$, is defined as RIm for convenience. Of triethylamine 1 equiv was added to each sample to deprotonate this ligand (see Experimental Section). [c] ImH = imidazole, $C_3H_4N_2$. [d] Bis(ImH) complex produced by addition of 100-fold excess of ImH. [e] 1 equiv of ImH plus 2 equiv of triethylamine (total). [f] 1 equiv of ImH plus 10 equiv of Proton Sponge. [g] 100 equiv of each of ImH and triethylamine. [h] g_x calculated assuming $g_z^2 + g_y^2 + g_x^2 = 16.0$. [i] Not observed at 77 K.

effect of deprotonation of imidazoles (designated ImH by them for clarity) on visible and EPR spectra.[67] While some of our results are in agreement with theirs, others are not: The two major points of disagreement are (1) the precise g values reported and (2) the g values of the neutrally charged monoimidazolate complex. The first point of disagreement is not important unless one wishes to compare exact g values between the two studies—the trends observed are the same. For identical systems in the same solvent (CH_2Cl_2), for example $(TPP)Fe(NMeIm)_2^+$, the earlier study reports $g_z = 2.92$, $g_y = 2.30$, $g_x = 1.55$[67] whereas we find $g_z = 2.87$, $g_y = 2.29$, $g_x = 1.56$. This amounts to a field sweep range difference of 3.4% in the two EPR spectrometers utilized. Similar differences are present in the parameters of the bis(imidazole) and bis(imidazolate) complexes. We have, in fact, applied a field sweep range correction of −3.2% to all of our EPR spectra, based upon field calibration using an NMR gaussmeter. Had we not applied this correction, our EPR parameters would be in close agreement with those of Quinn, Nappa, and Valentine.[67] Thus, although the reported values of rhombicity and tetragonality differ slightly in some cases, the conclusion still stands that the bis(imidazolate) complex is much more tetragonal (i.e., a stronger σ donor[9,19,21,67]) than the bis(imidazole), bis(alkylimidazole), or mixed RIm, ImH complexes, all of which have very similar EPR parameters (Table VI). However, for the intermediate, neutrally charged complex, containing one covalently attached alkylimidazole and one hydrogen-bonded or (more likely) deprotonated N–H imidazole, the EPR parameters are distinctly different from those reported previously.[67] In our case the mixed ligand complex was produced by adding 2 equiv of triethylamine or 10 equiv of proton sponge to a solution of 1 equiv of the protonated mono-side-arm imidazole complex and 1 equiv of imidazole. In either case, the EPR parameters are intermediate between those of the bis(RIm) and bis(Im^-) complexes, rather than nearly identical with those of the bis(Im^-) complex, as reported previously.[67] By our calculation, this places the monoimidazolate complex close to the bis(imidazole) and bis(alkylimidazole) complexes in rhombicity and tetragonality, both within the "B" group of Blumberg and Peisach, while the bis(imidazolate) complex is well within the "H" group, as expected (Figure 7). However, the monoimidazolate complex of our study contains an alkylimidazole as the sixth ligand, which provides no possibility of ligand field or charge variation through H bonding. Thus, we may expect that monoimidazolate, monoimidazole (ImH) $(TPP)Fe^{III}$ complexes may form a continuum of variable tetragonality from 3.3 to 3.8, the latter value being that found for the bis(imidazolate) complex, depending upon the extent, or lack thereof, of H bonding of the bound imidazole (ImH) ligand to other species present in the solution. This extent may also vary with temperature, which may explain why the earlier study found the ImH, Im^- complex to have very similar EPR parameters to those of the bis(imidazolate) complex, even though the room-temperature electronic spectra differed.[67] Likewise, variation in the strength of H-bonding interactions within the various B and even H-type heme proteins listed in Table I may account for much of the observed variation in EPR parameters.

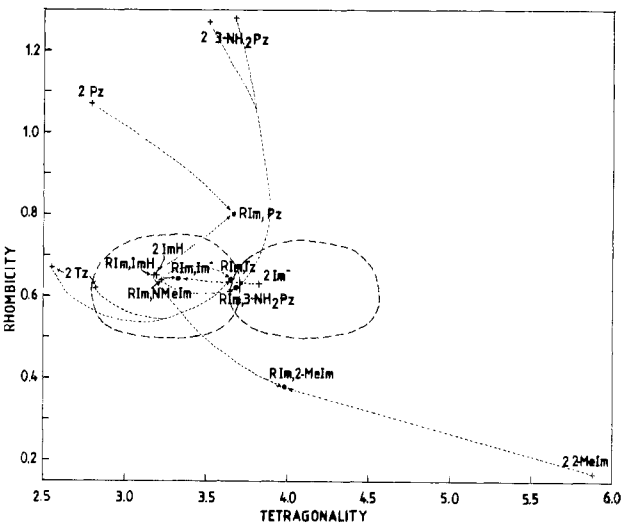

Figure 7. Plot of rhombicity (V/Δ) vs. tetragonality (Δ/λ) showing the values observed for low-spin mixed-ligand complexes of Fe^{III} TPPs.

Among the nonphysiological mixed-ligand complexes which can be produced from the mono-side-arm porphyrins, those involving one imidazole together with one pyrazole, one triazole, one 2-methylimidazole, or one 3-aminopyrazole show unique EPR parameters, different from those of any of the symmetrical bis-ligand complexes of which the mixed-ligand complexes are composed. The first three mixed-ligand complexes show significantly greater tetragonality than either symmetrical bis-ligand complex from which they are composed, while for the mixed-ligand complex with 3-aminopyrazole, the tetragonality is similar to that of the bis-(3-aminopyrazole) complex, while the rhombicity is similar to the bis(*N*-methylimidazole) complex. No quantitative explanation of these effects is offered here but rather simply the comment that there must be electronic synergism between the two unlike axial ligands which produces unique magnetic properties for Fe^{III}.

While certain of the above-mentioned mixed-ligand complexes are not expected to be physiologically significant, they raise the question as to the EPR parameters which might be expected for certain potentially physiological mixed-ligand complexes of iron(III) porphyrins. For example, several years ago a correlation was developed between the value of g_{max} (usually called g_1 or g_z, although the axis system is usually not known) and the nature of the two axial ligands bound to eukaryotic and prokaryotic cytochromes c as a function of pH.[39] For g_{max} greater than 3.2, the axial ligands were believed to be methionine + Im^- (3.2–3.26), ImH + aliphatic amine (3.33–3.41), Im^- + aliphatic amine (slightly larger), and two aliphatic amines (3.57–3.63).[39] It is also known that several mitochondrial cytochromes b and c have large values of g_{max}: beef heart mitochondria have large g_{max} assigned to cytochrome c_1 (3.33), b_K (3.44), and b_T (3.78).[35] By the classification system[39] discussed above, we would thus suspect that cytochrome c_1 has one protonated histitinde plus one aliphatic

amine, while cytochrome b_K probably has a deprotonated histidine plus one aliphatic amine, and cytochrome b_T probably has two aliphatic amines as axial ligands. However, Carter, Tsai, and Palmer[47] have recently pointed out that $g_{max} = 3.40$ can be obtained from solutions of protoporphyriniron(III) bound to two 2-methylimidazole ligands, thus calling into question the classification system developed prev'ously.[39] In addition, ferricytochrome a_3 of bovine heart mitochondrial cytochrome oxidase, when bound to cyanide, while Cu_{a_3} is bound to NO, yields two different "strong g_{max}" signals, depending on whether NO is added to partially ($g_{max} = 3.58$)[98] or fully ($g_{max} = 3.40$)[99,100] oxidized, CN^--bound cytochrome oxidase. These species clearly do not conform to the ligand classification system[39] discussed above, since one of the heme ligands is cyanide.

Spectra with a strong $g_{max} = 3.4$ (Figure 3b) can be produced with $(TPP)Fe^{III}$ bound to two hindered imidazoles, two low basicity pyridines, and similar strong g_{max} signals, but centered at $g = 2.6$, are found with two hindered pyrazoles or with two benzotriazoles (see Table III). All of these signals are observed only at temperatures below 30 K, and all have the same strong g_{max} and nearly undetectable g_2 and g_3. The shapes are anomalous for rhombic EPR signals and may possibly arise from significant g strain in these systems.[101] Interestingly, our mixed-ligand complexes containing one RIm and one 2-MeIm or one 3,4-lutidine (Table VI) have intermediate shapes (g_{max} not as strong as that of Figure 3b, g_2 detectable, at least for the 2-MeIm mixed-ligand complex, at 77 K). Unfortunately, it has not been possible to obtain the EPR spectra of model compounds containing two aliphatic amines or one aliphatic amine and one RIm bound to the axial positions of iron(III) porphyrins due to autoreduction of Fe^{III} in the presence of aliphatic amaines containing protons.[97] Since the interpretation of the EPR and Mössbauer spectra of the species shown in Figure 3b is still in progress,[68] we are not yet in a position to say what factors lead to the signal of Figure 6b, which is the only feature observed for the large g_{max} signals of the mitochondrial cytochromes.[35,95-100] However, the fact that the nonphysiological mixed-ligand complexes of Table VI (RIm–pyrazole, RIm–3-aminopyrazole, or RIm–1,2,4-triazole) do not have EPR parameters which are the average of the symmetrical bis-ligand complexes of which they are composed suggets that considerable additional study of low-spin iron(III) porphyrins is needed in order to reliably assign the axial ligands present in membrane-bound cytochromes *b* and *c* and to understand the nature of the cyanide-bound hemin a_3 signal of cytochrome oxidase.[98-100]

Note Added in Proof. Widger and co-workers[102] have recently reported the amino acid sequences of cytochromes *b* of complex III from five different mitochondrial sources and a chloroplast cytochrome b_6, which all appear to have two hemes, each bound to two histidine imidazoles. The two hemes appear to reside on opposite sides of the hydrophobic membrane core.[102] These hemes are those designated b-562 or b_K and b-566 or b_T, respectively.[35,102] Thus, the two histidine imidazoles of b_T and b_K must be in some unique orientation not shown by nonhindered imidazole complexes of model hemes in order to produce the observed large values of g_{max}.[35] Scheidt[103] has recently pointed out the extreme sensitivity of the magnetic properties of bis-aromatic amine complexes of iron(III) porphyrins to the orientation of the axial imidazoles. It is possible that the explanation of the large g_{max} signals may lie in the angular orientation of the axial ligands with respect to each other and/or the porphyrin ring.

Acknowledgment. The financial support of NIH (RCDA GM-00227 and AM-31038) and NSF (CHE 79-18217 and 75-20123) is gratefully acknowledged. Methods of separation of the mono- and dinitro $(TPP)H_2$ precursors of the aminoporphyrins used to synthesize the mono and biscovalently attached imidazole (TPP)Fe(III) complexes were developed by Dr. Robert S. McLeod. The 3,5-dimethyl-4-(dimethylamino)pyridine was prepared by Ava Finkel and the 3-methyl-4-(dimethylamino)-pyridine by Sarah Hall. $((Piv)_4TPP)FeCl$ isomers were prepared by Joanne Buehler and Joyce West. Part of this work was the M.S. research project of David Reis. The authors wish to thank Professor B. H. Huynh for many helpful comments.

Registry No. $(TPP)Fe(Im)_2Cl$, 25442-52-8; $(TPP)Fe(Im)_2I$, 92055-70-4; $(TPP)Fe(4\text{-}MeIm)_2Cl$, 61056-84-6; $(TPP)Fe(4\text{-}MeIm)_2I$, 92055-71-5; $(TPP)Fe(N\text{-}MeIm)_2Cl$, 41121-76-0; $(TPP)Fe(N\text{-}MeIm)_2I$, 61056-83-5; $(TPP)Fe(4\text{-}NMe_2Py)_2I$, 63832-67-7; $(TPP)Fe(4\text{-}NH_2Py)_2I$, 63832-68-8; $(TPP)Fe(3,4\text{-}(NH_2)_2Py)_2I$, 92055-72-6; $(TPP)Fe(3\text{-}Me,4\text{-}NMe_2Py)_2I$, 92055-73-7; $(TPP)Fe(3,5\text{-}Me_2,4\text{-}NMe_2Py)_2I$, 92055-74-8; $(TPP)Fe(3,4\text{-}Me_2Py)_2I$, 92055-75-9; $(TPP)Fe(Py)_2I$, 63832-70-2; $(TP\text{-}P)Fe(L)_2I$ (L = isoquinoline), 92055-76-0; $(TPP)Fe(Prz)_2I$, 92055-77-1; $(TPP)Fe(2\text{-}MePrz)_2I$, 92055-78-2; $(TPP)Fe(Pym)_2I$, 92055-79-3; (TPP)Fe(Pdz)I, 92055-80-6; $(TPP)Fe(3\text{-}MePdz)_2I$, 92055-81-7; $(TP\text{-}P)Fe(L)_2I$ (L = phthalazine), 92055-82-8; $(TPP)Fe(Trz)_2I$, 92055-83-9; $(TPP)Fe(N\text{-}bzlIm)_2I$, 92055-84-0; $(TPP)Fe(4\text{-}PhIm)_2I$, 92055-85-1; $(TPP)Fe(5\text{-}Cl,N\text{-}MeIm)_2I$, 92055-86-2; $(TPP)Fe(2\text{-}MeIm)_2I$, 92055-87-3; $(TPP)Fe(5,6\text{-}Me_2bzlIm)_2I$, 92055-88-4; $(TPP)Fe(1,2\text{-}Me_2Im)_2I$, 92055-89-5; $(TPP)Fe(3\text{-}NH_2Pz)_2I$, 92078-31-4; $(TPP)Fe(5\text{-}NH_2Iz)_2I$, 92055-90-8; $(TPP)Fe(6\text{-}NH_2Iz)_2I$, 92055-91-9; $(TPP)Fe(3\text{-}MePz)_2I$, 92055-92-0; $(TPP)Fe(4\text{-}IPz)_2I$, 92055-93-1; $(TPP)Fe(Pz)_2I$, 92055-94-2; $(TPP)Fe(Iz)_2I$, 92055-95-3; $(TPP)Fe(3,5\text{-}Me_2Pz)_2I$, 92055-96-4; $(TP\text{-}P)Fe(L)I$ (L = *s*-triazolo[3,4-2]quinoline), 92055-99-7; $(m\text{-}F)(m\text{-}NO_2)_3TPPFe(N\text{-}MeIm)_2^+$, 80641-84-5; $(m\text{-}CH_3)(m\text{-}NO_2)_3TPPFe(N\text{-}MeIm)_2^+$, 80641-82-3; $(p\text{-}COOEt)_4TPPFe(N\text{-}MeIm)_2^+$, 92056-00-3; $(m\text{-}NO_2)(m\text{-}F)_3TPPFe(N\text{-}MeIm)_2^+$, 92078-32-5; $(m\text{-}Cl)_4TPPFe(N\text{-}MeIm)_2^+$, 92078-33-6; $(p\text{-}CONMe_2)_4TPPFe(N\text{-}MeIm)_2^+$, 92078-34-7; $(p\text{-}CONH(CH_2)_3CH_3)_4TPPFe(N\text{-}MeIm)_2^+$, 92078-35-8; $(m\text{-}F)_4TPPFe(N\text{-}MeIm)_2^+$, 92078-36-9; $(p\text{-}Cl)_4TPPFe(N\text{-}MeIm)_2^+$, 80631-17-0; $(p\text{-}NO_2)(H)_3TPPFe(N\text{-}MeIm)_2^+$, 80641-68-5; $(m\text{-}NO_2)(H)_3TPPFe(N\text{-}MeIm)_2^+$, 80641-69-6; $(m\text{-}NO_2)(m\text{-}CH_3)_3TPPFe(N\text{-}MeIm)_2^+$, 80641-80-1; $(p\text{-}OCH_3)(p\text{-}Cl)_3TPPFe(N\text{-}MeIm)_2^+$, 80641-88-9; $(p\text{-}NO_2)(p\text{-}CH_3)_3TPPFe(N\text{-}MeIm)_2^+$, 80641-81-2; $(m\text{-}NHCOCH_3)(H)_3TPPFe(N\text{-}MeIm)_2^+$, 80641-78-7; $(m\text{-}OCH_3)(H)_3TPPFe(N\text{-}MeIm)_2^+$, 80641-72-1; $(p\text{-}NEt_2)(p\text{-}Cl)_3TPPFe(N\text{-}MeIm)_2^+$, 80641-63-0; $TPPFe(N\text{-}MeIm)_2^+$, 52155-25-6; $(p\text{-}NHCOCH_3)(H)_3TPPFe(N\text{-}MeIm)_2^+$, 80641-77-6; $(p\text{-}OCH_3)(p\text{-}F)_3TPPFe(N\text{-}MeIm)_2^+$, 80641-86-7; $(p\text{-}CN)(p\text{-}OCH_3)_3TPPFe(N\text{-}MeIm)_2^+$, 92078-37-0; $(p\text{-}OCH_3)(H)_3TPPFe(N\text{-}MeIm)_2^+$, 80641-71-0; $(m\text{-}CH_3)_4TPPFe(N\text{-}MeIm)_2^+$, 92078-38-1; $(p\text{-}Cl)(p\text{-}OcH_3)_3TPPFe(N\text{-}MeIm)_2^+$, 80641-87-8; $(p\text{-}NH_2)(H)_3TPPFe(N\text{-}MeIm)_2^+$, 80641-74-3; $(p\text{-}CH_3)_4TPPFe(N\text{-}MeIm)_2^+$, 92078-39-2; *trans*-$(p\text{-}NEt_2)_2(p\text{-}Cl)_2TPPFe(N\text{-}MeIm)_2^+$, 80641-64-1; *cis*-$(p\text{-}NEt_2)_2(p\text{-}Cl)_2TPPFe(N\text{-}MeIm)_2^+$, 80641-65-2; $(p\text{-}OCH_3)_4TPPFe(N\text{-}MeIm)_2^+$, 82781-61-1; $(p\text{-}Cl)(p\text{-}NEt_2)_3TPPFe(N\text{-}MeIm)_2^+$, 80641-66-3; $(p\text{-}NEt_2)_4TPPFe(N\text{-}MeIm)_2^+$, 80641-67-4; *trans*-$((ImCH_2CH_2OCONH)_2TPP)FeCl$, 92078-40-5; *cis*-$((ImCH_2CH_2OCONH)_2TPP)FeCl$, 92078-41-6; $((o\text{-}NHCOC(CH_3)_3)_4TPP)FeCl$, 92078-42-7; (TPP)Fe(RIm)(NMeIm)Cl, 92078-43-8; (TPP)Fe(RIm)(ImH)Cl, 92078-44-9; (TPP)Fe(ImH)-(ImH)Cl, 92096-17-8; $(TPP)Fe(RIm)(Im^-)$, 92078-45-0; (TPP)Fe-(RIm)(Pz)Cl, 92078-46-1; $(TPP)Fe(RIm)(3\text{-}NH_2Pz)Cl$, 92078-47-2; (TPP)Fe(RIm)(2-MeIm)Cl, 92078-48-3; $(TPP)Fe(RIm)(L_2)Cl$ (L_2 = 3,4-lutidine), 92078-49-4; $(TPP)Fe(3\text{-}NH_2,1,2,4\text{-}Tz)_2I$, 92055-97-5; $(TPP)Fe(1,2,4\text{-}Tz)_2I$, 92055-98-6.

(98) Johnson, M. K.; Eglinton, D. G.; Gooding, P. E.; Greenwood, C.; Thomson, A. J. *Biochem. J.* **1981**, *193*, 699–708.
(99) Brudvig, G. W.; Stevens, T. H.; Morse, R. M.; Chan, S. I. *Biochemistry* **1981**, *20*, 3912–3921.
(100) Hill, B. C.; Brittain, T.; Eglinton, D. G.; Gadsby, P. M. A.; Greenwood, C.; Nicholls, P.; Peterson, J.; Thomson, A. J.; Woon, T. C. *Biochem. J.* **1983**, *215*, 57–66.
(101) Pilbrow, J. R., personal communication.
(102) Widger, W. R.; Cramer, W. A.; Herrmann, R. G.; Trebst, A. *Proc. Natl. Acad. Sci. U.S.A.* **1984**, *81*, 674–678.
(103) Geiger, D. K.; Lee, Y. J.; Scheidt, W. R. *J. Am. Chem. Soc.* **1984**, *106*, 6339–6343.